1996

Nitrogen Release during Coal Combustion

Thomas H. Fletcher
Brigham Young University, tom_fletcher@byu.edu

Larry L. Baxter
Brigham Young University

Reginald E. Mitchell
Sandia National Labs

Robert H. Hurt
Sandia National Labs

Original Publication Citation

Baxter, L. L., R. E. Mitchell, T. H. Fletcher, and R. H. Hurt, "Nitrogen Release during Coal Combustion," Energy and Fuels, 10, 188-196 (1996). DOI: 10.1021/ef9500797

Release of Inorganic Material During Coal Devolatilization

LARRY L. BAXTER,* REGINALD E. MITCHELL,† and THOMAS H. FLETCHER‡
Combustion Research Facility, Sandia National Laboratories, Livermore, CA 94551-0969

Experimental results presented in this paper indicate that coal devolatilization products convectively remove a fraction of the nonvolatile components of inorganic material atomically dispersed in the coal matrix. Results from three facilities burning six different coals illustrate this mechanism of ash transformation and release from coal particles. Titanium is chosen to illustrate this type of mass release from coal particles on the basis of its low volatility and mode of occurrence in the coal. During moderate rates of devolatilization (10^4 K/s heating rate), no significant loss of titanium is noted. At more rapid rates of heating/devolatilization (10^5 K/s) a consistent but minor (3%–4%) loss of titanium is noted. During rapid devolatilization (5×10^5 K/s and higher), significant (10%–20%) amounts of titanium leave the coal. The loss of titanium monitored in coals ranging in rank from subbituminous to high-volatile bituminous coals and under conditions typical of pulverized-coal combustion. The amount of titanium lost during devolatilization exhibits a complex rank dependence. These results imply that other atomically dispersed material (alkali and alkaline earth elements) may undergo similar mechanisms of transformation and release.

INTRODUCTION

Among the issues determining the design, operation, and efficiency of past and present coal conversion technologies, the behavior of mineral matter plays a significant, some say dominant, role [1]. Development of new coal conversion technology will undoubtedly benefit greatly from an improved understanding of this issue. Recent literature documents progress toward this goal [2–7]. While experimental and theoretical approaches differ, these investigations reach the consensus that a general understanding of inorganic behavior requires consideration of the mineralogy and modes of occurrence of the coal inorganic material in addition to its elemental composition. This is in contrast to 'indices' of coal behavior that rely on algebraic relationships between elemental descriptions of the coal inorganic material. Also, the transformations of this inorganic material during combustion are as important in determining the fate of the material as is the elemental composition. Unlike the elemental composition, these transformations depend on the temperature and composition of the environment through which the particle passes.

Granular minerals dominate the inorganic material of most bituminous and many subbituminous coals and lignites. Inorganic material atomically dispersed in the coal matrix or dissolved in pore water occurs in increasing amounts in U.S. coals with decreasing coal rank. We refer to both types of material as inorganic matter in this discussion. The term *mineral matter* refers to actual minerals that are granular but may or may not be crystalline. The term *ash* refers to the product of the inorganic material after combustion and applies to both entrained particles (fly ash) and ash deposits. Inorganic matter within a coal particle has one of two fates. It either contributes to the formation of a residual fly ash particle or leaves the original coal particle in the form of a gas or a condensed phase.

The two mechanisms most commonly indicated in the literature by which inorganic material leaves a particle are fragmentation and vaporization [8–21]. In this context, fragmentation includes shedding of surface particles during combustion, collapse of char structures into several individual pieces, and physical fracturing of individual inorganic mineral grains resulting in formation of separate fly ash particles. Vaporization, in this context, refers to the formation of a near-equilibrium gas partial pressure of a species over its condensed phase

*Corresponding author: Larry Baxter, P.O. Box 969/7011 East Avenue, Sandia National Laboratories, Livermore, CA 94551-0969.
†Currently at High Temperature Gas Dynamics Laboratory; Stanford University; Palo Alto, CA 94305.
‡Currently at Chemical Engineering Department; Brigham Young University; Provo, UT 84601.

COMBUSTION AND FLAME 108:494–502 (1997)

Published by Elsevier Science Inc.
0010-2180/97/$17.00
SSDI 0010-2180(95)00120-U

and the subsequent transport of this species into the bulk gas stream. Other investigators have documented the loss of nonvolatile materials, including titanium, from coal during rapid heating (10^5–10^6 K/s) high temperature (2000–2800 K) devolatilization experiments. These experiments combined relatively inert particles with pulverized coal particles and based mass balances on the concentration of inert particles in the sampled solids [22]. The extent to which material was released from the particles discussed in this paper increased monotonically with increasing particle burnout. All inorganic material inherent in the coal was released to a measureable extent.

Recent experiments indicate an additional mechanism for the release of material from pyrite and other reactive inorganic grains [23]. These experiments, coupled with observations of inorganic grain fragmentation during particle heating and reaction [24], indicate that under some conditions the granular inorganic material may contribute more significantly to the small portion of the particle size distributions than previously recognized.

The results reported below indicate that another additional mechanism of mass release from coal during combustion, primarily involved with the atomically dispersed or very fine-grained inorganic material, complements those discussed above. The mechanism involves the convective transport and removal of atomically dispersed or fine-grained inorganic material during coal devolatilization. In the discussion below, analyses of nonvolatile, atomically dispersed or fine-grained material (titanium) inherent in the coal illustrate this mechanism and its dependence on coal type and rate of devolatilization.

EXPERIMENTAL EQUIPMENT, MATERIALS, AND PROCEDURES

The experimental facilities used in this investigation include the coal devolatilization laboratory (CDL), the coal combustion laboratory (CCL), and the multifuel combustor (MFC). All are located at the Combustion Research Facility of Sandia National Laboratories. These facilities are described in some detail in the literature [23, 25, 26]. They provide a capability to study the effect of devolatilization rate on mineral matter transformations over a wide range of controlled conditions. A brief, functional description of the facilities and their capabilities, as used in this investigation, is given here.

The CDL includes a laminar, electrically heated flow reactor and an in situ, particle-sizing, two-color pyrometer. The flow reactor entrains size- and aerodynamically classified samples of coal. An isokinetic, helium-quench probe samples the entrained particles at residence times up to about 300 ms. The pyrometer system obtains single-particle temperature, velocity, and size measurements at each sampling location. Inductively coupled atomic absorption spectroscopy characterizes the elemental composition of the inorganic constituents of the particles. Additional analyses characterize the elemental compositions of the organic portion, particle density and pore size distributions, surface areas, etc. Maximum gas temperatures vary up to approximately 1250 K, producing initial particle heating rates up to about 10^4 K/s. Particles are injected at room temperature and experience an initial rapid increase in temperature. Maximum particle temperatures attained in the CDL are approximately 1150 K. Inert gas environments used in the flow section and sampling systems of the CDL, preclude oxidation of the samples.

The CCL resembles the CDL in design and scale. The primary differences involve the vitiated, oxygen-bearing flow in the CCL. The vitiated flow of the CCL allows initial particle heating rates as high as 5×10^5 K/s and, consequently, more rapid rates of devolatilization than are obtained in the CDL. Initial gas temperatures reach approximately 1800 K in all experiments. Particles combust in two environments, one containing 6 and the other 12 mol.% oxygen. Otherwise, the gas environments are identical. Particles enter the reactor at room temperature. Maximum particle temperature attained in the CCL is approximately 1950 K and particle residence times are as long as 150 ms.

The MFC simulates conditions in a commercial-scale boiler. Utility-grind coal (70% through 200 mesh) is used in the facility and particle residence times of 3 s or longer are

obtainable. Mass-average particle diameters are 20–30 μm. Firing rates and particle loadings in the MFC are matched to those of commercial-scale boilers. Gas and particle temperatures and heatup rates are also chosen to match those of commercial-scale boilers. Maximum particle temperatures exceed 2000 K. In most experiments, devolatilization rates in the MFC exceed those in either the CDL or CCL.

All three laboratories capture solid samples from the reacting flow using Nuclepore polycarbonate filters with 1 μm openings and total diameters of either 76 or 142 mm. The sampling efficiency of particles greater than 1.2 μm in diameter exceeds 99.9% whereas the sampling efficiency of particles less than 0.8 μm in diameter is less than 0.1%. This filtration system separates particles on the basis of their absolute, as opposed to aerodynamic, diameters. The collection system in the CDL separates tars from solid particles prior to collecting the solid particles on the filter.

Both size-classified and utility-grind samples of pulverized coal were used in these experiments. The CDL and CCL use exclusively size-classified samples whereas the MFC uses utility grind coal (Fig. 1). In all cases, the elemental concentrations of the organic and inorganic components were established by replicate ASTM analyses of the raw coal. The results of primary interest are the measured mass fraction of titanium, silicon, and aluminum in the coal and char as a function of particle residence time.

Silicon and aluminum are used as tracers to identify the overall rate of mass release from the coal. In the case of the CCL, the ratio of the mass fed to the mass extracted from the combustor is also used to compute the overall mass loss. This procedure cannot be used in the CDL, where tar condensation and collection prevent a meaningful measurement, or in the MFC, where the entire flow stream is not sampled. The agreement between the mass balance and tracer results using aluminum and silicon in the CCL is excellent.

Titanium, which is known to occur in coal in both mineral and atomically dispersed forms [27], is used as a representative atomically dispersed element. Titanium is chosen from

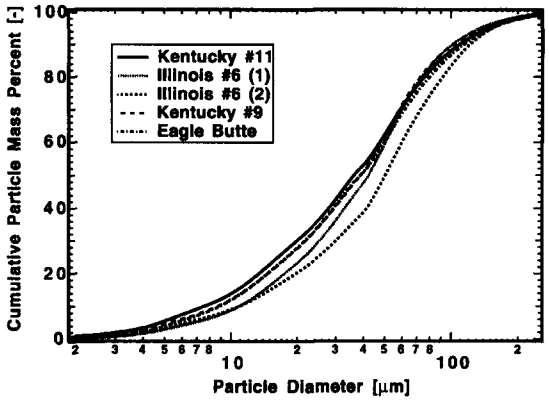

Fig. 1. Particle size distributions of the five utility grind coals used in the MFC. Each curve indicates the mass of total coal with a diameter below the given value. Data are derived from both optical and sieve techniques. All coals meet the typical boiler specification of 70% through 200 mesh (70% less than 74 μm).

among other atomically dispersed elements because in virtually all of its forms its vapor pressure at combustion temperatures is very low. Because of this low vapor pressure, classical chemical vaporization is an unlikely explanation for its release from coal particles. The mode of occurrence of atomically distributed titanium in coal is most commonly as a complex with oxygen, but occasionally as an organically bound material [27]. There is no clear indication of rank dependence in the amount of atomically dispersed titanium found in the coal.

Two size ranges of an Illinois #6 hvc bituminous coal (PSOC-1493D) were used in the CCL and CDL under several operating conditions during this investigation. Five additional utility-grind coals were used in the MFC. The mass percent of all inorganic species relevant to this investigation (silica, alumina, titania, and ash) in the raw coal particles is indicated in Table 1 for both size ranges. The data are reported on a dry, whole-coal basis and represent the average of several replicated measurements. Note that there are several coals in the table that are named Illinois #6. These are from different mines and have different properties, as indicated. Numbers in parenthesis are used to distinguish them. The elemental composition of the raw coals and of the solid samples collected from the three reactors was

TABLE 1

Concentrations of Silicon, Aluminum, and Titanium (Expressed as Oxides) and Total Ash in the Raw Coals Used in this Investigation (all results are for utility grind coals except where size ranges are specified)

Coal	SiO_2 (% of dry coal)	Al_2O3 (% of dry coal)	TiO_2 (% of dry coal)	Oxygen (% of dry coal)	Total Ash (% of dry coal)
Illinois #6 (PSOC 1493d) 75–106 μm	3.61	1.43	0.088	10.5	11.83
Illinois #6 (PSOC 1493d) 106–125 μm	4.23	1.68	0.092	11.9	11.85
Kentucky #11	10.14	4.14	0.19	8.25	22.21
Illinois #6 (1)	6.10	2.31	0.11	8.86	12.33
Kentucky #9	6.59	2.97	0.15	9.07	14.64
Illinois #6 (2)	4.7	1.71	0.090	10.19	10.13
Eagle Butte	1.79	0.91	0.054	20.18	6.4

determined using inductively coupled plasma/atomic absorption spectroscopy.

The fractional loss of any element from the particle at time i is determined from a combination of the overall mass loss and the change in the mass fraction of that element, as follows

$$R_j(t) = 1 - (m(t)/m_o)\big(x_j(t)/x_{oj}\big), \qquad (1)$$

where R_j represents the cumulative fraction of the original mass of element j released from the particle up to time t, m is the overall mass of the particle, and x is the mass fraction of element j in the particle. Subscript o represents a value in the raw coal (residence time of 0 ms). All other values are time dependent, as indicated.

Overall mass loss is computed by averaging the results of tracer techniques and mass balances (where feasible). Silica and alumina were found to be the best tracers in most cases. Mass loss calculated from the concentrations of these materials in the coal were in close agreement with both each other and with the measured change in mass between coal and char samples. There was no indication of a change in the silica-to-alumina ratio during combustion. The variance of the overall mass loss was calculated from the independent measurements of mass loss (mass balance and tracers) and from replicated experiments. This variance is used to compute the variance for individual points.

Statistical variation in the value of R arises from sample-to-sample variations and experimental error in three experimentally determined values in Eq. 1: the overall mass loss at time $t(m(t)/m_o)$; the original fraction of element j in the coal particle (x_{oj}); and the time-dependent fraction of element j in a coal particle $(x(t)_j)$. The total variance in R at a given residence time can be estimated from these three sources as follows [28]:

$$\sigma_{R_j}^2 = \sigma_{m/m_o}^2\left(\frac{\langle x_j\rangle}{\langle x_{oj}\rangle}\right)^2 + \sigma_{x_j}^2\left(\left\langle\frac{m}{m_o}\right\rangle\frac{1}{\langle x_{oj}\rangle}\right)^2 + \sigma_{x_{oj}}^2\left(\left\langle\frac{m}{m_o}\right\rangle\frac{\langle x_j\rangle}{\langle x_{oj}\rangle^2}\right)^2, \qquad (2)$$

where angle brackets represent mean values, σ^2 represents a variance, and the remaining symbols have been previously defined. All quantities are time dependent except those bearing a subscript o. This approach can be used to estimate variances on a point-by-point basis. Variances in groups of data, i.e., all points after coal devolatilization, can be calculated using standard statistical techniques [29]. The statistical analyses of the data are based on these variances.

RESULTS AND DISCUSSION

Figures 2–4 illustrate the data and trends for the fractional overall mass loss (dashed lines

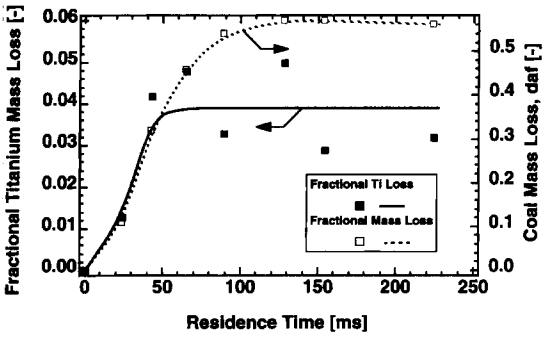

(a)

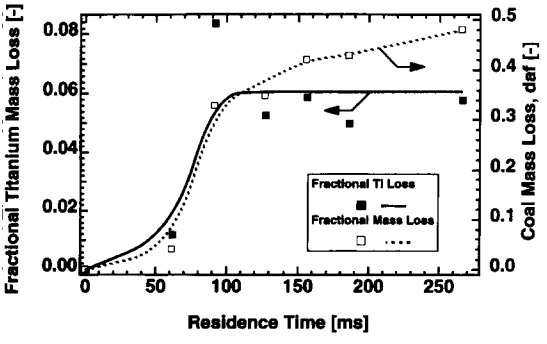

(b)

Fig. 2. Illustration of titanium mass loss at moderate rates of devolatilization. Data are collected from the CDL with maximum gas temperatures of: (a) 1050 K and (b) 1250 K. All data are for 75–106 μm size fraction of an Illinois #6 coal (PSOC 1493D).

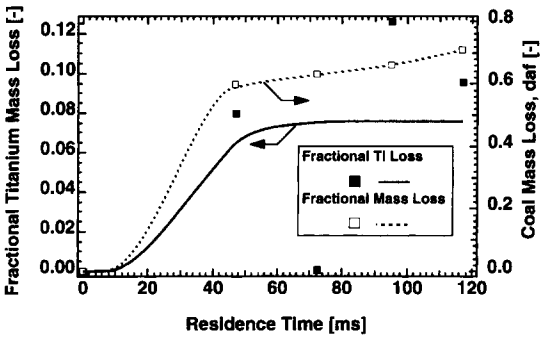

(a)

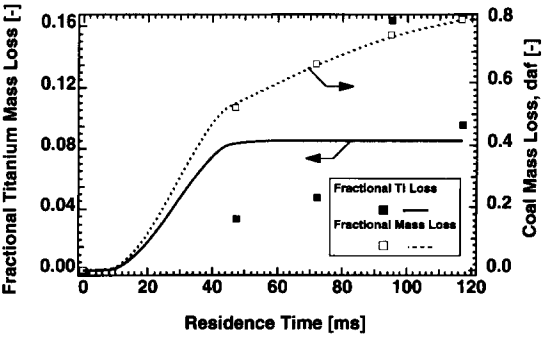

(b)

Fig. 3. Illustration of titanium mass loss at intermediate rates of devolatilization compared to Figs. 1 and 3. Data are collected from the CCL in gas environments containing: (a) 6 mole percent and (b) 12 mol.% oxygen. All data are for the 106–125 μm size fraction of an Illinois #6 coal (PSOC 1493D).

scaled by the right ordinate) and the fractional titanium loss (solid lines scaled by the left ordinate) as a function of particle residence time in the CDL and CCL. Because the CDL data are obtained in an oxygen-free environment, all of the mass loss indicated in Figs. 2a and 2b is attributable to devolatilization. The overall mass loss indicated in Fig. 3 includes both devolatilization and oxidation results. The separation between devolatilization and heterogeneous oxidation mass loss occurs at about 45 ms.

The least rapid rates of devolatilization among the data from the size-classified coals are experienced by the small (75–106 μm) particles in the CDL, where maximum gas temperatures range from 1050 to 1250 K. In these experiments, mass loss during devolatilization can be resolved. These are the only data presented that include solid samples collected during devolatilization.

The data illustrated in Fig. 3 were collected in the CCL under conditions of more rapid devolatilization than is attained in the CDL. The data differ only in the bulk gas oxygen composition, with results from environments containing 6 and 12 mol.% oxygen being presented in Figs. 3a and 3b, respectfully. The difference in gas composition has little impact on the rate of devolatilization. The bulk gas temperatures in the 6% and 12% oxygen environments are essentially identical and the particles are not exposed to oxygen during devolatilization due to the combustion of the surrounding volatile cloud. Therefore, the differences in the rates of devolatilization are minimal in these two gas environments.

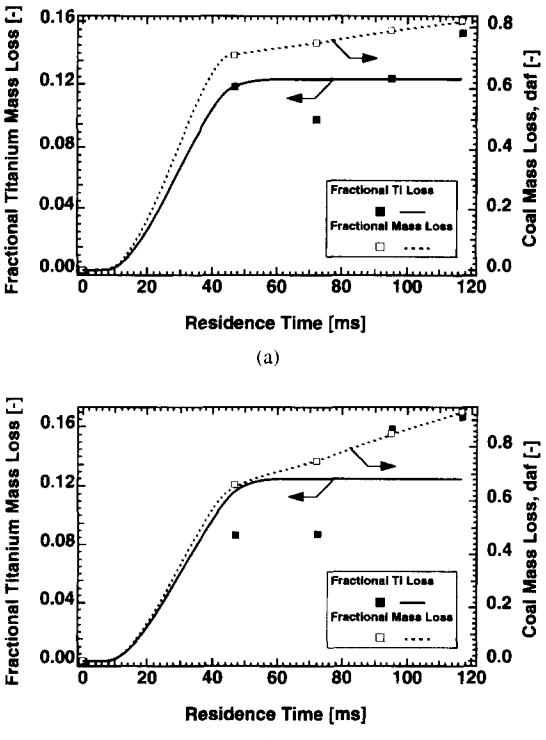

Fig. 4. Illustration of fractional titanium mass loss at rapid rates of devolatilization compared to Figs. 1 and 2. Data are collected from the CCL in gas environments containing: (a) 6 mol.% and (b) 12 mol.% oxygen. All data are for the 106–125 μm size fraction of an Illinois #6 coal (PSOC 1493D).

The data illustrated in Fig. 4 were collected under conditions inducing the most rapid rates of devolatilization among the CCL and CDL data sets. Again, the difference in the two figures is the bulk oxygen concentration in the gas under the conditions of the experiment.

These data will be used to illustrate a correlation between the rate of coal devolatilization and loss of titanium from the coal. The curves in Figs. 2–4 represent overall mass and overall titanium release. The curves themselves are drawn to aid the eye and do not represent correlations or theory. All of the mass release data are on a dry, ash-free basis and lie very close to the line. The titanium data inherit the uncertainty in the mass loss data and that of several other chemical analyses (see Eq. 2). The increased scatter in the titanium data relative to the mass loss data reflect this variation. The solid curve representing overall titanium release reaches a plateau shortly after devolatilization stops. This plateau is the calculated average value of all data points after the end of devolatilization in each experiment.

The most obvious and important trends indicated by the data are (1) a small fraction of the titanium leaves the coal during devolatilization and (2) the amount of titanium leaving the coal generally increases with increasing rate of devolatilization. The CDL data indicate that an average of five percent of the titanium is released during devolatilization. The data at intermediate rates of devolatilization, i.e., from the large particles in the CCL (Fig. 3), indicate an average of eight percent titanium leaving the particle. And the data at the most rapid rates of devolatilization in the CCL (Fig. 4) indicate an average of 12% titanium leaving the coal particle.

Release of titanium by vaporization cannot satisfactorily explain this loss of titanium. The common forms of titanium in coal are less volatile than the common forms of either silicon or aluminum, yet the titanium is leaving the coal particles whereas silicon and aluminum are not. Vaporization should be most rapid at peak particle temperatures. These occur after coal devolatilization, where the rate of titanium loss has become essentially zero. Also, the rate of vaporization from a given sample of coal should be determined primarily by the particle temperature history. These data indicate a more sensitive dependence on devolatilization rate than on temperature history. For example, compare the data in Figs. 3 and 4, all of which have virtually identical gas temperature histories but which represent two different devolatilization rates.

We propose convective transport by coal volatiles as a more satisfactory explanation for these data. Elucidation of the details of this mechanism will require additional careful experimentation. These data, however, provide direct support for the overall features of mineral matter release by coal devolatilization and a foundation from which hypotheses can be generated. Coal devolatilization is, on a particle scale, the most rapid reaction experienced by the particles during combustion. At conditions typical of commercial pulverized coal combustion, the rate of devolatilization ex-

ceeds that of the experiments illustrated by the data in Figs. 2–4. During this rapid reaction, organically associated material and possibly very fine particulate are locked into organic structures that are undergoing pyrolysis. This material is carried into the bulk gas stream with the volatiles, not because of its inherent volatility, but rather because of its intimate association with reacting coal matrix.

This mechanistic hypothesis explains the trend of increasing loss of material with increasing rate of devolatilization. This trend, with statistical confidence limits, is illustrated in Fig. 5a. A detailed analysis of the confidence limits on a point-by-point basis using Eq. 2 indicates that only those data derived from experiments with many replicates and under conditions of rapid devolatilization or highest titanium mass loss can be demonstrated to be statistically significant, i.e., 95% confidence limits for the mean that exclude zero mass loss. This results primarily from the limited number of effective replicate experiments under identical conditions at the same residence time. However, if the data collected before and after devolatilization are considered as two groups, we can demonstrate statistically that they have different degrees of titanium loss.

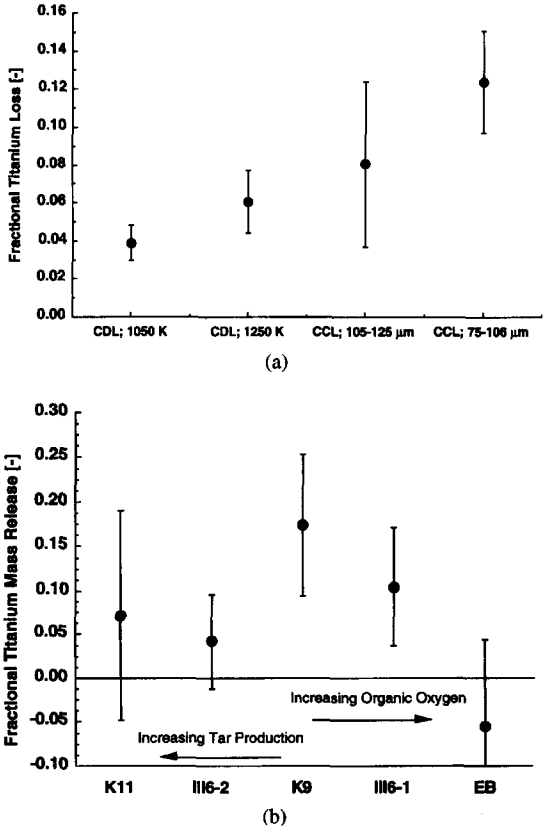

Fig. 5. Comparison of titanium mass before and after devolatilization for data collected from: (a) the CDL and CCL; and (b) the MFC. Data are plotted in order of: (a) increasing rate of devolatilization and (b) decreasing rank. Error bars represent 95% confidence limits.

Figure 5a indicates the average and 95 percent confidence intervals for the fraction of titanium released from coal during devolatilization under each of the essentially equivalent conditions indicated in Figs. 2–4. In Fig. 5a, the data from the CDL at each gas temperature condition and the data from the CCL for each different particle size are arranged in order of increasing rate of devolatilization. The first two points summarize data from the same size fraction of the same coal collected in the same reactor (CDL) at different gas temperatures. Therefore, the bulk gas temperature, or rate of devolatilization, is the dominant difference in the data. As indicated, the amount of titanium lost increased with increasing rate of devolatilization. The last two points summarize data collected from the CCL. In this case, the rate of devolatilization has been controlled by changing particle size. All of the data, including those collected at the most moderate rates of devolatilization, indicate a statistically significant loss of titanium during devolatilization, with the amount lost increasing with increasing rate of devolatilization.

Similar data for a several additional coals tested in the MFC are presented Fig. 5b in rank order. The mass-average rate of devolatilization for the data from the MFC exceeds that of both the CCL and the CDL. However, because a utility grind coal was used in the MFC experiments, particle heating and devolatilization rates span a broad range in these results. The data indicate a complex rank dependence of titanium release. The Illinois #6 coal used in the CCL and CDL experiments ranks between the Kentucky #9 and Illinois #6 (2) coals indicated in Fig. 5(b).

As a practical consideration, the relevance of these results rests in their implication for materials that are bound in coal in a similar

fashion as titanium but that play a more significant role in determining things such as ash deposit tenacity and strength in commercial combustion systems. Condensation of vapors during deposition is implicated in the formation of unmanageable, tenacious, strong deposits on boiler heat transfer surfaces. Inorganic materials likely to condense during combustion have their origin primarily as atomically dispersed species in the coal, with sodium being the most notable example and the remaining alkali and alkaline earth elements also implicated. The classical volatility of some of these species, most importantly sodium, precludes their use to distinguish classical vaporization from convective transport during devolatilization. However, there is an obvious implication from the results of the nonvolatile titanium species for the remaining atomically dispersed material. Namely, if titanium is effectively transported by this mechanism, all other atomically dispersed species potentially could experience a similar fate.

CONCLUSIONS

Coal devolatilization at rates typical of pulverized coal combustors induces a mineral matter release mechanism that is characterized by convective transport of organically-bound and possibly small-grained material away from the coal particle. This mechanism is experimentally demonstrated for titanium for a variety of devolatilization rates (heating rates) and a variety of coal types. The extent of loss of titanium varies from zero to over 16% of the original titanium mass. The extent of titanium loss depends most strongly on particle heating and devolatilization rate, organically associated oxygen, and extent of tar production. These tendencies support the proposed mechanism of titanium release as relating to the atomically dispersed inorganic material convectively carried out of the coal particle.

These data indicate that the mechanism of convective transport during coal devolatilization contributes to the formation of inorganic vapors and fumes during coal combustion. This additional mechanism of mineral matter release should be considered when describing the chemical composition of fly ash particles and the amount of condensible material formed during combustion.

This work was supported by the U.S. Department of Energy through the Pittsburgh Energy Technology Center's Direct Utilization Advanced Research and Technology Development Program. The authors acknowledge the contributions of Ephraim Arquitola, Scott Ferko, and Al Salmi in operating and maintaining the several experimental facilities used in these experiments. The contributions of visiting students and teachers, most notably Eric Harwood, Joe Stieve, and James Brandt, are similarly recognized. The contribution of Don Hardesty as a technical reviewer of this work and as the project manager largely responsible for the development of the coal-related research at Sandia is gratefully acknowledged. All of the experimental work indicated in this paper was performed in the Combustion Research Facility of Sandia National Laboratories.

REFERENCES

1. Raask, E., *Mineral Impurities in Coal Combustion*, Hemisphere, Washington, 1985.
2. Borio, R. W., and Levasseur, A. A., *Eighth Annual International Pittsburgh Coal Conference*, The University of Pittsburgh, 1991.
3. Brekke, D. W., Zygarlicke, C. J., Folkedahl, B. C., and Steadman, E. N., *Eighth Annual Pittsburgh Coal Conference*, The University of Pittsburgh, 1991, pp. 12–18.
4. Baxter, L. L., and DeSollar, R. W., *Fuel*, in press.
5. Barta, E. L., Toqan, M. A., Beér, J. M., and Sarofim, A. F., *Eighth Annual International Pittsburgh Coal Conference*, 1991.
6. Srinivasachar, S., Helble, J. J., and Boni, A. A., *Twenty-Third Symposium (International) on Combustion*, The Combustion Institute, Pittsburgh, 1990, pp. 1305–1312.
7. Srinivasachar, S., Senior, C. L., Helble, J. J., and Moore, J. W., *Twenty-Fourth Symposium (International) on Combustion*, The Combustion Institute, Pittsburgh, in press.
8. Helble, J. J., Neville, M., and Sarofim, A. F., *Twenty-First Symposium (International) on Combustion*, The Combustion Institute, Pittsburgh, 1986, pp. 411–417.
9. Flagan, R. C., *Seventeenth Symposium (International) on Combustion*, The Combustion Institute, Pittsburgh, 1978, pp. 97–104.
10. Schulz, E. J., Engdahl, R. B., and Frankenbuerg, T. T., *Atmos. Environ.* 9:111–119 (1975).
11. Markowski, G. R., Ensor, D. S., Hooper, R. G., and Carr, R. C., *Environ. Sci. Technol.* 14:1400–1402 (1980).
12. Taylor, D. D., and Flagan, R. C., *Aerosol Sci. Technol.* 1:103–117 (1982).

13. Neville, M., Quann, R. J., Haynes, B. S., and Sarofim, A. F., *Eighteenth Symposium (International) on Combustion*, The Combustion Institute, Pittsburgh, 1980, pp. 1267–1274.
14. Neville, M., and Sarofim, A. F., *Fuel* 64:384–390 (1985).
15. Ramsden, A. R., *Fuel* 48:121–137 (1969).
16. Sarofim, A. F., Howard, J. B., and Padia, A. S., *Combust. Sci. Technol.* 16:187–204 (1977).
17. Desrosiers, R. E., Riehl, J. W., Ulrich, G. D., and Chiu, A. S., *Seventeenth Symposium (International) on Combustion*, The Combustion Institute, Pittsburgh, 1978, pp. 1395–1403.
18. Linak, W. P., and Peterson, T. W., *Twenty-First Symposium (International) on Combustion*, The Combustion Institute, 1986, Pittsburgh, pp. 399–410.
19. Kang, S.-G., Helble, J. J., Sarofim, A. F., and Beér, J. M., *Twenty-Second Symposium (International) on Combustion*, The Combustion Institute, Pittsburgh, 1988, pp. 231–238.
20. Schafer, H. N. S., *Fuel* 58:667–672 (1979).
21. Schafer, H. N. S., *Fuel* 58:673–679 (1979).
22. Gat, N., Cohen, L. M., Witte, A. B., and Denison, R. M., *Combust. Flame* 57:255–263 (1984).
23. Baxter, L. L., and Mitchell, R. E., *Combust. Flame* 88:1–14 (1992).
24. Baxter, L. L., *Prog. Ener. Combust. Sci.* 16:261–266 (1990).
25. Fletcher, T. H., *Combust. Flame* 78:223–236 (1989).
26. Baxter, L. L., *Combust. Flame* 90:174–184 (1992).
27. Finkelman, R. B., Ph.D. dissertation, University of Maryland, 1980.
28. Papoulis, A., *Probability, Random Variables, and Stochastic Processes*, McGraw-Hill series in electrical engineering, *Communications and Information Theory*, McGraw-Hill, New York, 1984.
29. Canavos, G. C., *Applied Probability and Statistical Methods*, Little, Brown, Boston, 1984.

Received 31 March 1992; revised 5 May 1995